



SEISMIC FRAGILITY ANALYSIS OF RC STRUCTURES: USE OF RESPONSE SURFACE FOR A REALISTIC APPLICATION

P. FRANCHIN¹, A. LUPOI¹, P.E. PINTO², M.IJ. SCHOTANUS³

SUMMARY

A statistical approach for seismic reliability problems is applied in the assessment of an RC frame structure. The procedure establishes a response surface, characterised by a statistical model of the mixed type, to represent the seismic capacity in an analytical limit-state function. The fragility function of the system is then calculated by FORM analysis, with the constructed empirical limit-state function as input. The application concentrates on the clarification of implementation issues, and confirms the versatility of the method in realistic problems.

INTRODUCTION

Reinforced concrete structures can fail according to a wide variety of modes: flexural deformation failure of members in bending, shear failure of columns, tensile or compressive joint failure among others. The capacity models for all these failure modes are characterised by a fairly high degree of (epistemic) uncertainty, mainly due to a yet incomplete knowledge of the underlying behaviour, especially where complex interaction phenomena are concerned, e.g. the one between shear, torsion and bending. This uncertainty adds to the one arising from the inherent randomness in the material properties. An equal level of uncertainty is present in the response (demand) analysis.

A response surface approach arises as a natural choice to lighten the computational burden when these capacity and demand models enter in reliability analysis. In the model used, which has been already extensively validated (Franchin [1,2]), the failure probability is expressed, following a well-established format in earthquake engineering, as a function of the earthquake intensity only, i.e. as a fragility function. The method is here applied in the assessment of a real three-storey 3D RC structure, designed solely for gravity loads according to the design and construction practice of the early 70's in southern Europe. Actual test data are available, and the probabilistic assessment is compared with the real behaviour of the structure.

¹ Research fellow, Dept. of Structural & Geotechnical Engineering, Univ. of Rome "La Sapienza", Italy.
Email: paolo.franchin@uniroma1.it

² Professor, Dept. of Structural & Geotechnical Engineering, Univ. of Rome "La Sapienza", Italy.

³ PhD Candidate, European School for Advanced Studies in Reduction of Seismic Risk (ROSE School), Pavia, Italy.

PROBABILISTIC ASSESSMENT PROCEDURE

Statement of the seismic reliability problem

Let \mathbf{x} be a $k \times 1$ random vector completely characterised by its joint probability density function $f(\mathbf{x})$, whose components can be of load or resistance type. In the space of \mathbf{x} a limit-state function (LSF) is defined, usually indirectly in terms of the response of the structure $r(\mathbf{x})$, as a scalar function $g[r(\mathbf{x}), \mathbf{x}]$ that takes on positive values as long as the structure is safe in the corresponding failure mode, and negative values when it has failed, the boundary $\{\mathbf{x} | g[r(\mathbf{x}), \mathbf{x}] = 0\}$ between the two conditions being called limit-state surface.

For seismic problems the response, and possibly the LSF itself, need to be described as functions of time t . This requires that the LSF is re-written as time-dependent: $g[r(\mathbf{x}, t), \mathbf{x}, t]$. The reliability is therefore also time-dependent, and can be expressed as:

$$\Pr \left\{ \min_{t \in [0, T]} g[r(\mathbf{x}, t), \mathbf{x}, t] < 0 \right\} \quad (1)$$

where in $t = 0$ a safe state is assumed, and T is the time interval of interest (the duration of a seismic event). Using Eq. 1, the fragility is defined as:

$$\Pr \left\{ \min_{t \in [0, T]} g[r(\mathbf{x}, t), \mathbf{x}, t] < 0 | IM \right\} \quad (2)$$

i.e. as the failure probability conditional to an intensity measure (IM) characterising the ground-motion. Following current practice, the spectral acceleration for the fundamental period of the structure, $S_a(T_1)$, is used for this purpose.

When dealing with RC structures, the response in the inelastic range, that is necessary for the evaluation of LSF's representing collapse, generally requires a demanding numerical (finite element) time-history analysis, corresponding to a realisation of \mathbf{x} . In order to solve Eq. 2, it is then often necessary to pass to the computationally expensive class of *simulation methods*. In that case, reduction of the effort associated with these latter is mandatory if realistically complex systems are to be considered.

A factor that has large impact in decreasing the required number of simulations is the choice of the form of the LSF. Typically it is put in a *capacity (C) minus demand (D)* format. The dimensionally homogenous quantities C and D then represent response values such as bending moments, displacements etc., as needed in the criteria defining the various failure modes. One effective formulation, after Veneziano [3], is obtained by expressing both capacity and demand in terms of spectral acceleration:

$$g(\mathbf{x}) = S_{a;C}(\mathbf{x}) - S_{a;D} \quad (3)$$

where $S_{a;C}(\mathbf{x})$ represents the spectral acceleration for which the maximum response in time reaches the limit-state, and $S_{a;D}$ is the demand spectral acceleration. The fact that $S_{a;D}$ is a parameter implies that once an analytical expression for the capacity $S_{a;C}(\mathbf{x})$ has been formulated, one can build the entire fragility solving the problem repeatedly, changing the value of $S_{a;D}$.

The format is generalised to the system case by defining:

$$S_{a;C}(\mathbf{x}) = \min_m \{ S_{a;C_m}(\mathbf{x}) \} \quad (4)$$

i.e. taking $S_{a;C}(\mathbf{x})$ as the lowest value of the m distinct failure modes that leads to system failure. This means that failure is assumed to be attained as soon as the structure fails according to any of the included failure modes, which is equivalent to considering a series system. The most important feature of using the

formulation in Eq.s 3 and 4 is that a unique LSF is used irrespective of the number m of failure modes and that the interaction between the failure modes is implicitly accounted for.

Within this framework, the *response surface technique* will be employed as a means to obtain an analytical approximation for the capacity term $S_{a;c}(\mathbf{x})$ with a limited number of simulations. The constructed response surface is then used as input for FORM analysis to calculate fragility values.

Mixed-model response surface

Let now \mathbf{x} be a $k \times 1$ vector of *controllable* basic variables. Let Y be a *measurable* random variable, representing $S_{a;c}(\mathbf{x})$, whose mean value is believed to depend, in an unknown fashion, on the quantities collected in \mathbf{x} . Let $\mu_Y(\mathbf{x})$ be a model of this dependence. Let one further assume that Y can be expressed in the additive form:

$$Y(\mathbf{x}) = \mu_Y(\mathbf{x}) + \varepsilon \quad (5)$$

where ε is a random deviation term with zero-mean, called error term, assumed as Gaussian distributed, that gives account of the random variability of Y around its true mean, as well as of the inadequacy of the mean model $\mu_Y(\mathbf{x})$ to represent the relation between the true mean and \mathbf{x} , also due to the limited statistical information from which its parameters are estimated.

Establishing an empirical/analytical model of the dependence of the response Y on \mathbf{x} such as that represented by Eq. 5 is the aim of the response surface technique, and comprises three stages: the choice of the model; the collection of data in the form of $\{Y, \mathbf{x}\}$ pairs, from carefully planned simulations (using notions from the branch of statistics called *experimental design*); the estimation of the model parameters (using the techniques of *statistical inference*). Each of these issues is addressed extensively in Franchin [1,2], and is briefly summarised in the following.

As far as the choice of the model for $\mu_Y(\mathbf{x})$ is concerned, linear or quadratic models of Y in \mathbf{x} are classically postulated that explicitly relate Y to the components of \mathbf{x} through a number of unknown model parameters. Since the size of the experimental basis needed to estimate these parameters grows rapidly with increasing size of \mathbf{x} , cases with more than six variables are rarely found in the applied statistical literature.

As an adequate mathematical description, even in its most simplified form, requires the introduction of a large number of random variables (in the order of hundreds-of-thousands, e.g. random amplitudes and phases in a spectral representation, random pulses in a time-domain representation), it is out of the question to *explicitly* account for the dependence of Y on all variables needed to describe earthquake loading.

The alternative is to account for their effect in a global, *implicit*, way. To this end the vector \mathbf{x} is partitioned into two sub-vectors \mathbf{x}_1 and \mathbf{x}_2 , collecting the few variables whose effect is modelled explicitly and those many whose effect is modelled globally, respectively. The \mathbf{x}_2 sub-vector thus represents uncertainty related to the earthquake, and its implicit effect is modelled resorting to the concept of *random factors* (Searle [4]). These latter are physical factors that randomly affect the response, assumed to do so in an additive manner. The corresponding *mixed type* response model is:

$$Y(\mathbf{x}_1, \mathbf{x}_2) = \mathbf{z}(\mathbf{x}_1)\boldsymbol{\beta} + \delta + \varepsilon \quad (6)$$

where $\mathbf{z}(\mathbf{x}_1)\boldsymbol{\beta}$ is called the *fixed-effect* part of the model, while δ is the *random-effect*, i.e. the effect of the random factor \mathbf{x}_2 . The fixed-effect part of the model defines a classical response surface, i.e. a linear combination of p generally non-linear functions of \mathbf{x}_1 , usually referred to as *explanatory* functions:

$$\mathbf{z}(\mathbf{x}_1)\boldsymbol{\beta} = \sum_{i=1}^p \beta_i z_i(\mathbf{x}_1) \quad (7)$$

where $\mathbf{z}(\mathbf{x}_1)$ is the $1 \times p$ row vector of explanatories, and $\boldsymbol{\beta}$ collects the p model parameters. For what concerns the random factor effect, making the common assumption that δ is a zero-mean Gaussian variable, the only unknown is its variance σ_δ^2 .

The design of experiments to provide data for the estimation of the model in Eq. 6 is a delicate issue. A convenient experimental plan for producing data to estimate the parameters of a quadratic surface is the *central composite design* (CCD), which consists of a complete *two-level factorial design* augmented with a *star design* (Box [5]). The former consists of taking two levels (low, $\xi = -1$, and high, $\xi = +1$) for each of the basic variables and performing an experiment for every one of the 2^k resulting combinations. The star design adds two additional points at level $\xi = \pm\alpha$ (with $\alpha > 1$, see for example Box [5]) for each basic variable in \mathbf{x}_1 plus n_0 centre points (at level $\xi = 0$), resulting in a total of $n = 2^k + 2k + n_0$ experiments. In this case, where the basic variables are random variables with a known distribution, a convenient choice is to define $\xi = (x - \mu)/\sigma$ (Cochran [6]).

The CCD allows estimation of the parameters of the fixed effect part only, and a modification is necessary to also allow estimation of the random factor effects. One attractive and well-established technique, called *blocking of the experiments*, provides a solution to this problem (Box [5]). It is historically used when the experiments cannot be carried out in homogeneous conditions, for instance because there is some uncontrollable and unknown source of heterogeneity and the effect of this latter has to be determined in order to discount it. Here the situation is reversed, and the experiments are carried out purposely introducing the source of heterogeneity (different earthquake records), to be able to determine its contribution to the variability of Y , represented by δ .

If the n experiments are grouped (*blocked*) into b blocks with n_i experiments each, and to each block a different ground-motion record is assigned, i.e. the dynamic finite element analysis is carried out with that record as input, the results of the n experiments can be collectively written in matrix form as:

$$\mathbf{Y} = \mathbf{Z}\boldsymbol{\beta} + \mathbf{B}\boldsymbol{\delta} + \boldsymbol{\varepsilon} \quad (8)$$

where $\boldsymbol{\delta}$ is a $b \times 1$ vector that collects the *block effects*, i.e. the random (factor) effects, and \mathbf{B} is a $n \times b$ matrix that collocates each random effect to the correct block of experiments:

$$\mathbf{B} = \begin{bmatrix} \mathbf{1}_{n_1} & \mathbf{0}_{n_1} & \cdots & \mathbf{0}_{n_1} \\ \mathbf{0}_{n_2} & \mathbf{1}_{n_2} & \cdots & \mathbf{0}_{n_2} \\ \vdots & \vdots & \ddots & \vdots \\ \mathbf{0}_{n_b} & \mathbf{0}_{n_b} & \cdots & \mathbf{1}_{n_b} \end{bmatrix} \quad (9)$$

where $\mathbf{1}_{n_i}$ and $\mathbf{0}_{n_i}$ are vectors of length n_i made up of ones and zeroes, respectively. The block effects collected in $\boldsymbol{\delta}$ are a finite number of observations of the random variable δ , from which the distribution of the latter is estimated. All other symbols in Eq. 8 have the same meaning as before.

While for the classical response surface the model parameters $\boldsymbol{\beta}$ are obtained from Ordinary Least Squares estimation independent of the error term variance, for the model given in Eq. 7 this is not possible: the parameters $\boldsymbol{\beta}$ have to be estimated together with the variances σ_δ^2 and σ_ε^2 . This is necessary because the experiments are no longer uncorrelated. In fact, from the model given in Eq. 8 one has:

$$\mathbf{C}_{\mathbf{Y}\mathbf{Y}} = \mathbf{E}[(\mathbf{Y} - \boldsymbol{\mu}_{\mathbf{Y}})(\mathbf{Y} - \boldsymbol{\mu}_{\mathbf{Y}})^T] = \mathbf{E}[(\mathbf{B}\boldsymbol{\delta} + \boldsymbol{\varepsilon})(\mathbf{B}\boldsymbol{\delta} + \boldsymbol{\varepsilon})^T] = \mathbf{B}\mathbf{B}^T \sigma_{\boldsymbol{\delta}}^2 + \mathbf{I}\sigma_{\boldsymbol{\varepsilon}}^2 \quad (10)$$

where $\mathbf{B}\mathbf{B}^T$ is a non-diagonal matrix.

Estimates of $\boldsymbol{\beta}$, $\sigma_{\boldsymbol{\delta}}^2$ and $\sigma_{\boldsymbol{\varepsilon}}^2$ can be obtained by Maximum Likelihood estimation using the likelihood function:

$$L(\boldsymbol{\beta}, \mathbf{C}_{\mathbf{Y}\mathbf{Y}} | \mathbf{Y}) = f(\mathbf{Y} | \boldsymbol{\beta}, \mathbf{C}_{\mathbf{Y}\mathbf{Y}}) = |\mathbf{C}_{\mathbf{Y}\mathbf{Y}}|^{-\frac{1}{2}} \exp\left[-(\mathbf{Y} - \mathbf{Z}\boldsymbol{\beta})^T \mathbf{C}_{\mathbf{Y}\mathbf{Y}}^{-1} (\mathbf{Y} - \mathbf{Z}\boldsymbol{\beta})\right] \quad (11)$$

whose maximisation is a constrained optimisation problem since $\sigma_{\boldsymbol{\delta}}^2$ and $\sigma_{\boldsymbol{\varepsilon}}^2$ must both be positive.

APPLICATION

The method described in the previous section is here applied in the fragility analysis of a real three-storey 3D RC structure (Figs 1-2), designed solely for gravity loads according to the design and construction practice of the early 1970's in southern Europe, i.e. including plan irregularity and strongly eccentric beam-column connections, added to overall poor local detailing, scarcity of rebars, insufficient confinement, weak joints and older construction practice.

The building has been designed, studied, constructed and pseudo-dynamically tested under bi-directional loading within the framework of the EU funded SPEAR project (Kosmopoulos [7], Negro [8]). It has been purposely designed to exhibit all the failure modes typical to non-seismically designed structures, and thus it was expected to experience flexural yielding at the bottom and top of the square columns, in particular at the first floor, together with bar-slippage in the area of lap splicing at the bottom of first and second floor columns.

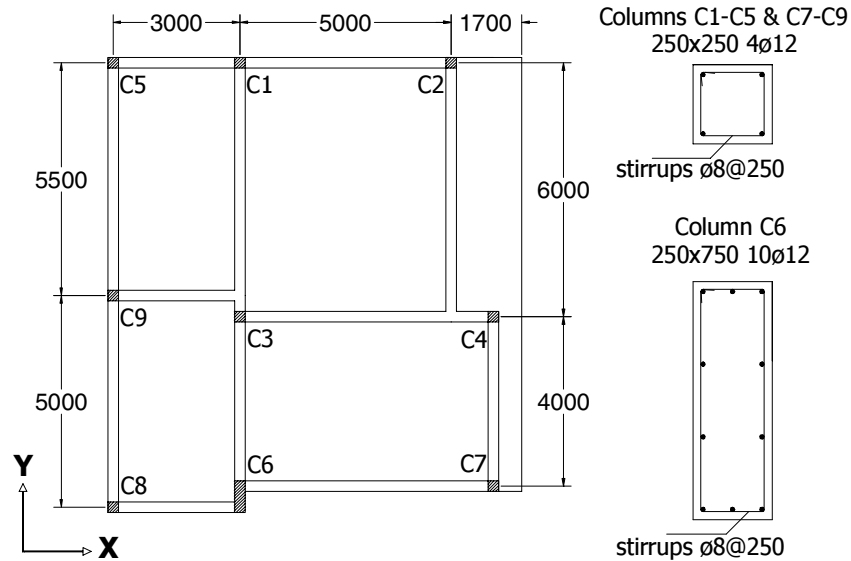


Figure 1. Plan view of the structure with details of column cross-sections (dimensions in [mm])



Figure 2. Photo of full scale model as built

The application described here is aimed at showing the potentiality of the procedure discussed in the previous section in a realistic situation. The fragility analysis carried out takes into account all the indications of previous research concerning the random factor representing uncertainty due to earthquake loading (Franchin [2]). Data required for the assessment, both in terms of capacity models and section modelling, are taken from *fib* Bulletin 24, “Seismic assessment and retrofit of reinforced concrete buildings” [9]. At the end of this section, a comparison is made with the outcome of the tests as carried out at the ELSA laboratory of the Joint Research Centre in Ispra, Italy (Negro [8]).

Mechanical parameters influencing the response

Only a limited number of variables, taking account of the effect of variations in the mechanical parameters on the response, can be introduced as explicit variables for the construction of the response surface. It is therefore convenient to work in the space of basic material properties, as they enable the description of sectional variability with a minimum of variables.

In this application, the variability in the response is assumed to be essentially influenced only by the concrete cylinder peak stress f_c and the steel yield stress f_y . These two variables describe the randomness of the material properties for the whole structure, i.e. their spatial variability throughout the structure is not considered.

In order to also account for this spatial variability, additional random-effect variables should be introduced (Franchin [1]). In this application a simpler approximate approach is adopted, consisting in inflating the variability of the steel yield strength by doubling its coefficient of variation (CoV), to account for variations in the amount of steel present in the section.

Following the recommendations of *fib* Bulletin 24 [9], the remaining parameters describing the constitutive behaviour of the unconfined and confined concrete on the section level are calculated using well-established relationships relating them directly to f_c , f_y and other section properties that are here considered as deterministic. A bi-linear steel model is fully determined by its yield strength f_y , and deterministic stiffness coefficients.

The mean values of the material properties considered are shown in Table 1, together with the values of the coefficient of variation typically associated with each of them. They are both assumed to be log-normally distributed.

Definition of capacity: failure modes of RC structures

As the frame under consideration is likely to fail due to the loss of load-bearing capacity of one or more columns, two relatively well established criteria are selected for flexural and shear failure of these structural members. Furthermore, as the joints are not reinforced, criteria for the joint shear capacity are also considered. Alternative modes of failure may be introduced, without affecting the general procedure.

Flexural failure

Failure in flexure is attained when the maximum core compression strain reaches the crushing limit $\varepsilon_{cc,u}$. The capacity is related to the basic variables through the confinement model in Paulay [10]:

$$\varepsilon_{cc,u} = \left(0.004 + a\varepsilon_{su} \frac{\rho_{s,tr} f_{yst}}{f_{cc}} \right) \cdot \varepsilon_{\varepsilon_{cc,u}} \quad (12)$$

where ε_{su} , $\rho_{s,tr}$ and f_{yst} are the rupture strain, volumetric ratio and yield stress of the confining steel and f_{cc} is the confined concrete peak stress. A modification for old-type columns as suggested by Panagiotakos [11] is made, using $a = 0.6$ instead of the original value of $a = 1.4$.

To account for uncertainty and incompleteness in Eq. 11, a model error term $\varepsilon_{\varepsilon_{cc,u}}$ is used. It is included in the vector \mathbf{x}_1 and its properties are given in Table 1.

Shear failure

A shear strength model suggested in Kowalsky [12] is used to assess the shear resistance of members. Use of this model is deemed appropriate, as it is one of the few that enables computation of the capacity under bi-axial loading. The model considers the shear capacity as the sum of three distinct components:

$$V = (V_c + V_s + V_p) \cdot \varepsilon_V \quad (13)$$

where V_c represents the strength of the concrete shear resisting mechanism, V_s the capacity attributed to the steel truss mechanism, and V_p a component attributed to the axial load.

In *fib* Bulletin 24 [9] this model, originally calibrated to circular columns, is evaluated using an extensive database of columns, finding a mean value of the ratio of experimental to calculated results equal to 0.86 for rectangular sections and a corresponding CoV of 26.1%. A model correction term, represented in Eq. 13 by ε_V , is therefore adopted and included in \mathbf{x}_1 . Its properties are given in Table 1.

Joint-panel shear failure

Following the *fib* Bulletin 24 [9], the joint resistance is specified directly in terms of diagonal principal stresses at the joint centre. This approach is considered more consistent with the underlying mechanics of the problem, as it illustrates in a transparent manner the influence of axial load acting on beams or columns on joint cracking and ultimate strength. This is especially true for the connections of the test structure, which lack special shear reinforcement, suggesting that failure is attained when cracking or crushing of the panel zone occur. In that case, diagonal tension cracking or crushing in compression may be assumed to occur in the joint if either one of the tensile or compressive principal stresses exceeds the following limits, respectively:

$$\sigma_{t,c} = \frac{n_z}{2} \pm \sqrt{\left(\frac{n_z}{2}\right)^2 + \nu^2} \quad \begin{cases} \leq 0.29\sqrt{f_c} & \text{(tension)} \\ \geq -0.5f_c & \text{(compression)} \end{cases} \quad (14)$$

where n_z is the compression stress due to vertical axial forces in the adjacent columns, and ν the joint shear stress.

Table 1: Properties of the basic random variables (x_i)

		Mean	Units	CoV
Material uncertainty	f_c	25	[MPa]	0.20
	f_y	450	[MPa]	0.20
Model uncertainty	$\epsilon_{\epsilon_{cc,u}}$	1		0.20
	ϵ_V	0.86		0.26

Further settings for the simulations

Following the guidelines for minimum number and size of the blocking, as discussed in Franchin [2], results in an experimental plan requiring 90 numerical simulations divided into 9 blocks, each associated with a specific accelerogram. Since the 3D frame requires ground-motion input in 2 directions, 9 two-component records are selected to be used in the analysis, given in Table 2.

Consistent with attenuation relationships used in hazard computation (see Sabetta [13]), which use the larger of the two horizontal components of the motion in the regression analysis for predictive equations of response spectra, the fragility is expressed in terms of the *larger* spectral acceleration of the two components, at the fundamental period of the structure. As the direction of the motion cannot be predicted, each pair of records is applied twice, first with the strongest one along axis X, and then along axis Y (see Fig. 1 for axis location). The *worst case* scenario is used in the final computation of the risk.

Regarding the choice of the period, a previous study (Franchin [2]) indicated that it should reflect to some extent the non-linear behaviour of the response. Therefore the period is determined from displacement time-histories for the mean structure (i.e. the structure characterised by mean material properties) subjected to a record scaled to lead it to incipient yielding. The characteristic period $T = 0.8s$ is chosen as the mean of the X and Y period, as collapse can occur with the stronger (and therefore characterising, as explained above) component in either direction.

A second order polynomial is developed on the four basic variables of Table 1:

$$\ln[S_{a;C}(f_c, f_y, \epsilon_{\epsilon_{cc,u}}, \epsilon_V)] = \beta_0 + \beta_1 f_c + \beta_2 f_y + \beta_3 \epsilon_{\epsilon_{cc,u}} + \beta_4 \epsilon_V + \beta_5 f_c^2 + \beta_6 f_y^2 + \beta_7 \epsilon_{\epsilon_{cc,u}}^2 + \beta_8 \epsilon_V^2 + \beta_9 f_c \epsilon_{\epsilon_{cc,u}} + \beta_{10} f_y \epsilon_{\epsilon_{cc,u}} + \beta_{11} f_c \epsilon_V + \beta_{12} f_y \epsilon_V + \delta_{eq} + \epsilon \quad (15)$$

where all linear and quadratic terms are retained, but the interaction terms between concrete and steel strength and between the model errors are omitted. Next to the error term ϵ one random factor δ_{eq} is included, representing the earthquake.

Table 2: Accelerograms used in numerical analyses

Name	Date	Station name	M	R	PGA	Td	S _a (T=0.8s)	
							comp.1	comp.2
	(m/d/y)			[km]	[g]	[s]	[g]	[g]
1 Friuli	05/06/76	Tolmezzo	6.5	37.7	0.351	36.32	0.542	0.357
2 Loma Prieta	10/18/89	Apeel 7 Pulgas	7.1	47.7	0.156	39.95	0.290	0.181
3 Victoria Mexico	06/09/80	Cerro Prieto	6.4	34.8	0.621	24.45	0.477	0.305
4 Spitak Armenia	12/07/88	Gukasian	7.0	30.0	0.199	19.90	0.436	0.166
5 Imperial Valley	10/15/79	Cerro Prieto	6.9	26.5	0.169	63.70	0.415	0.162
6 Coalinga	05/02/83	Parkfield - Vineyard Canyon 3W	6.5	32.3	0.137	40.00	0.262	0.256
7 Northridge	01/17/94	Sandberg - Bald Mtn.	6.7	43.4	0.098	40.00	0.255	0.123
8 Loma Prieta	10/18/89	Palo Alto Slac Lab.	7.1	35.6	0.278	39.57	0.394	0.360
9 Kobe	01/16/95	TOT	6.9	57.9	0.076	39.00	0.378	0.252

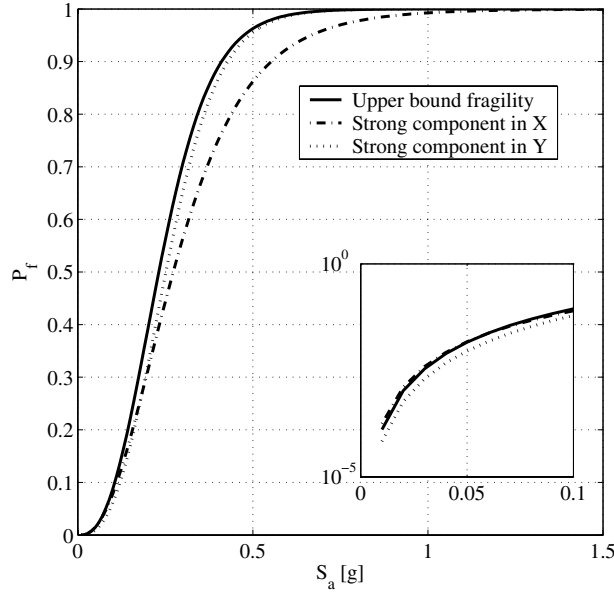


Figure 3. Fragilities obtained by considering different directions of loading

Results

Each experiment consists in repeatedly performing a time-history analysis for a realisation of the variables in \mathbf{x} scaling the associated accelerogram until the lowest of the capacity/demand ratios representing the several failure modes reaches unity. Once the $S_{a,C}(\mathbf{x})$ values for all the experiments are determined, the parameters of the response surface are computed with reference to the model described in Eq. 15, using Maximum Likelihood estimation. Subsequently, FORM analyses are carried out for a range of $S_{a,D}$ values to calculate the fragility, yielding the curves in Figure 3. Three fragilities are shown, one for the case in which the strongest (and characterising) component of the ground-motion is applied in the X direction, one when this component is applied in the Y direction, and finally one taking for each experiment the minimum $S_{a,C}$ of the two, indicated as *upper bound fragility*. This last one is used as the final fragility of the frame.

That the response surface is indeed a combined surface for multiple collapse mechanisms can be seen from Table 3, which reports the occurrences of the main failure modes for all 90 experiments that form the statistical basis of the final response surface. Modes 1 to 27 represent flexural failure in the columns: the first 9 for each of the corresponding columns of the first floor (Fig. 1), the second 9 (from 10 to 18) for each of the corresponding second floor columns, etc. Similarly, modes 28 to 54 represent the corresponding shear failure modes. Finally, modes 55 to 72 and 73 to 90 stand for joint-panel tension and compression failure respectively, e.g. mode 69 corresponds to joint-panel shear failure in tension of column C6 on the second floor.

Table 3: Modes determining collapse of the structure

Failure Modes	57	58	59	60	62	65	69	70
No. of failures	5	5	7	4	12	6	38	3

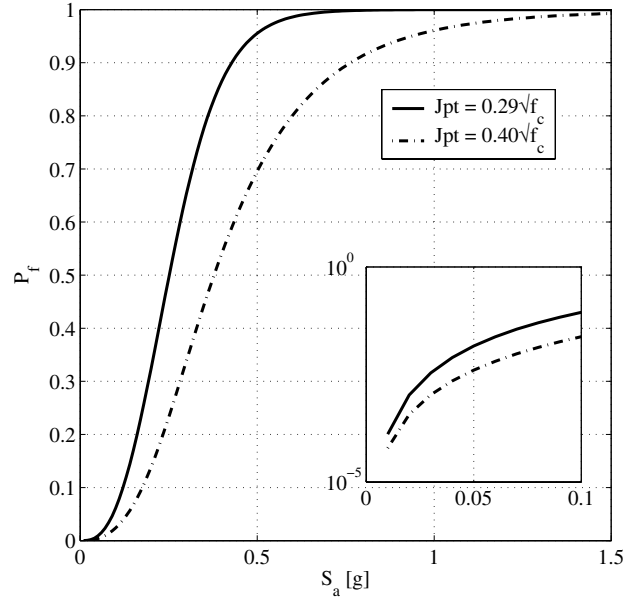


Figure 4. Fragility obtained considering higher joint-panel shear capacity

Discussion of results, comparison with test data and sensitivity analysis

Table 3 shows dominance of joint tensile failure, with the beam-column connections of column C8 (see Fig. 1) on the first floor and column C6 on the second floor accounting for over 50% of the failures. These results are apparently at difference with the results from the Pseudo Dynamic Tests, as reported in Negro [8], which, for a peak ground acceleration of 0.20g, showed spalling and flexural cracking at the top of the columns, with main damage concentrated at the top of the central column (C3) and at the flexible edge columns (C2, C4 and C7) of the second floor. Some damage was also detected in the beams and floor slabs connected to the strong column C6.

These results may indicate that the capacity values predicted by Eq. 14 underestimate the actual strength of the joint-panel in tension. When discussing the capacity criterion, *fib* Bulletin 24 [9] indicates various levels for the tension cracking. These levels are related to the type of confinement that characterises the joint, and vary from $0.2\sqrt{f_c}$ for T-joints with bar end hooks and smooth bars, to $0.42\sqrt{f_c}$ for T-joints with beam bars bent into the joint. However, these models have been calibrated using data from 2D tests, and thus do not give any indication of the favourable (or unfavourable) effect of the 3D configuration of the joints in the test structure. It is also noted that the floor slab of 150mm (30% of the beam height) will have a confining/stiffening effect on the joint region.

To examine the sensitivity of the results to the estimate of the joint capacity, the analyses are repeated using a value of $0.4\sqrt{f_c}$ for the joint tensile strength. For this case only the simulations in Y direction are performed, as Figure 3 indicates that the upper bound fragility is equal for practical purposes to the fragility with application of the strong component in Y direction. The resulting fragility function is shown in Figure 4.

Table 4: Risk values

	Risk
$J_{pt} = 0.29\sqrt{f_c}$	0.0238
$J_{pt} = 0.40\sqrt{f_c}$	0.0143

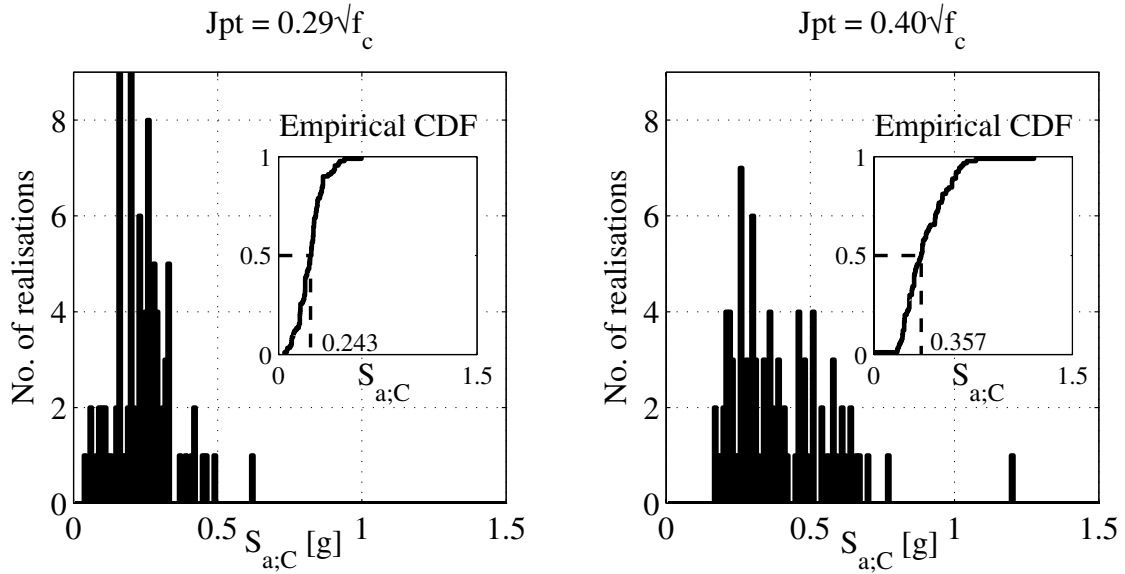


Figure 5. Distribution of $S_{a;C}$ for original (left) and modified (right) joint capacity

It appears that the relatively modest increase in the joint capacity leads to a considerably higher seismic resistance. This is confirmed by the $S_{a;C}$ values obtained from the simulations given in Figure 5, which show a shift of the capacity to higher values (the median goes up from 0.243g to 0.357g).

A more meaningful assessment of the sensitivity of the results to the changes in the model is represented by the value of the overall risk, given in Table 4, calculated from the convolution of the fragilities with a given hazard curve for a site in Southern Italy, representative of a zone with moderate to high seismic activity. It is noted that the influence on the risk is not such as to change its order of magnitude.

The results after modifying the joint tensile capacity also show a significant change in the distribution of the damage, as reported in Table 5. Failure is now concentrated in the central column (C3) and columns C2 and C4 of the flexible edge. Most of the other determining failure modes (6, 42, 60, 69) are related to flexural, shear and joint-panel failure of column C6 on the first and second floor. This indicates the vulnerability of the column, as is also seen from the test results. It might be concluded that efforts towards an improved modelling, in spite of the relatively small influence on the risk estimate, are of critical importance in the identification of more vulnerable elements and hence in the planning of upgrading interventions.

CONCLUSION

A statistical approach for seismic reliability problems was applied in the assessment of an RC frame structure. The procedure establishes a response surface, characterised by a statistical model of the mixed type, to represent the seismic capacity in an analytical limit-state function. The system fragility function is then calculated by FORM analysis, with the constructed empirical limit-state function as input.

Table 5: Modes determining collapse of the structure (modified joint strength)

Failure Modes	2	3	4	6	42	60	62	69
No. of failures	10	23	16	3	3	3	6	24

It was shown that the probabilistic procedure is *general* in the sense that it can be used in conjunction with state-of-the-art mechanical models, and that the variability in the response due to uncertainty in the input ground-motion is realistically represented. Further, variability of the mechanical parameters is included, and the computation of the failure probability can account for any type and number of different failure modes.

The application indicates that the method can be regarded as *affordable* as the number of computations can still be considered as acceptably low. The exact number of analyses needed is a function of the structure under consideration and of the iterative procedure used to arrive at failure. In the presented case study, for 90 experiments, the total number of simulation was 432 (an approximate average of 5 iterations per experiment).

Finally, the comparison made with actual test data shows the importance of representative capacity models and accurate FE modelling. Clearly, progress is still to be made in order to set up accurate and practical models that are able to reproduce the behaviour of poorly designed and detailed RC structures.

ACKNOWLEDGEMENTS

The work has been carried out under partial funding from the EU project SPEAR (Contract NG6RD-CT-2001-00525) and EU project SAFERR (Contract HPRN-CT-1999-00035).

REFERENCES

1. Franchin P, Lupoi A, Pinto PE, Schotanus MIJ. "Seismic fragility of reinforced concrete structures using a response surface approach." *Journal of Earthquake Engineering* 2003; 7 (Special Issue 1): 45-77.
2. Franchin P, Lupoi A, Pinto PE, Schotanus MIJ. "Response surface for seismic fragility analysis of RC structures." In: Der Kiureghian A, Madanat S, Pestana JM. (eds.). *Proceedings ICASP 9*. Rotterdam: Millpress, 2003: 41-48.
3. Veneziano D, Casciati F, Faravelli L. *Method of seismic fragility for complicated systems*. Proc. of the 2nd Committee of Safety of Nuclear Installation (CNSI) Specialist Meeting on Probabilistic Methods in Seismic Risk Assessment for NPP, Lawrence Livermore Laboratory, CA, 1983.
4. Searle SR, Casella G, McCulloch CE. "Variance components." N.Y.: John Wiley & Sons, 1992.
5. Box GEP, Draper NR. "Empirical model-building and response surfaces." N.Y.: John Wiley & Sons, 1987.
6. Cochran WG, Cox GM. "Experimental designs." (2nd ed.) New York: John Wiley & Sons, 1957.
7. Kosmopoulos A, Bousias SN, Fardis MN. "Design and pre-test assessment of 3-storey torsionally-unbalanced RC test structure." Paper No. 123, Proc. of fib 2003 Symposium: Concrete Structures in Seismic Regions, Athens, Greece, May 2003.
8. Negro P, Mola E, Molina JF, Magonette GE. "Full-scale bi-directional PsD testing of a torsionally unbalanced three-storey non-seismic RC frame." Proc. of the 13th World Conference on Earthquake Engineering, Paper N. 968, Vancouver, Canada, August 2004.
9. *fib*. "Seismic assessment and retrofit of reinforced concrete buildings." Bulletin 24, prepared by Task Group 7.1. Lausanne, 2003.
10. Paulay T, Priestley MJN. "Seismic design of reinforced and masonry buildings." N.Y.: John Wiley & Sons, 1992.
11. Panagiotakos TB, Fardis MN. "Deformations of reinforced concrete members at yielding and ultimate." *ACI Structural Journal* 2001; 98(2):135-148.
12. Kowalsky MJ, Priestley MJN. "Improved analytical model for shear strength of circular reinforced concrete columns in seismic regions." *ACI Structural Journal* 2000; 97(3): 388-396.
13. Sabetta F, Pugliese A. "Estimation of response spectra and simulation of nonstationary earthquake ground motions." *Bulletin of the Seismological Society of America* 1996; 8(2): 337-352.